



Minerva Access is the Institutional Repository of The University of Melbourne

Author/s:

Delgoda, DK;Saleem, SK;Halgamuge, MN;Malano, H

Title:

Multiple Model Predictive Flood Control in Regulated River Systems with Uncertain Inflows

Date:

2013-02-01

Citation:

Delgoda, D. K., Saleem, S. K., Halgamuge, M. N. & Malano, H. (2013). Multiple Model Predictive Flood Control in Regulated River Systems with Uncertain Inflows. *Water Resources Management*, 27 (3), pp.765-790. <https://doi.org/10.1007/s11269-012-0214-y>.

Persistent Link:

<https://hdl.handle.net/11343/282882>

Multiple Model Predictive Flood Control in Regulated River Systems with Uncertain Inflows

Dilini K. Delgoda · Syed K. Saleem · Malka N. Halgamuge · Hector Malano

Received: date / Accepted: date

Abstract This paper presents a novel approach to real time automatic flood control in a managed river network that is subject to uncertain inflows. The proposed approach uses multiple models to represent inflows ranging from low to high flow. Optimal model selection is achieved in a minimum mean square error sense using a bank of Kalman filters to identify the most likely inflow characteristic. There are no a-priori probabilities assigned to the individual models. Model Predictive Control is used for water level controller design. Our Adaptive Multi Model Predictive Control (AMMPC) method is proposed as an alternative to existing techniques that also use multiple inflow models but with a-priori inflow model probabilities, either weighted or equally likely. The performance of the approach is demonstrated using a simulated river-reservoir model as well as using data collected at the Wivenhoe Dam during the 2011 floods in Queensland, Australia.

Keywords Disturbance Rejection, Multivariable control systems, Model Based Control, Uncertainty

1 Introduction

Flooding in river systems is a common problem that has severe social, economic and environmental consequences. Flood management is a complex task that is usu-

Dilini K. Delgoda
Department of Infrastructure Engineering, The University of Melbourne, Parkville, VIC 3010, Australia
Tel.: +61433311624
E-mail: d.delgoda@pgrad.unimelb.edu.au

Syed K. Saleem
NICTA-Victorian Research Laboratory, The Univ. of Melb., Parkville, VIC 3010, Australia
Malka N. Halgamuge
Department of Electrical and Electronic Engineering, The Univ. of Melb., Parkville, VIC 3010, Australia
Hector Malano
Department of Infrastructure Engineering, The Univ. of Melb., Parkville, VIC 3010, Australia

ally addressed by in-stream storage reservoirs to buffer excess inflow and hydraulic structures (gates) to control the rate of discharge in the river network after periods of heavy rainfall. This infrastructure is typically managed using rule based methods that rely on local river operators' experience and judgment [21,35]. The main disadvantage of these approaches is that they are usually based on water level measurements in reservoirs and do not systematically take into account future predictions of rainfall and the resultant catchment inflows.

Time series modeling has been successfully applied to predict streamflow based on precipitation measurements in the catchment [37,42]. A successful approach incorporates parallel models which capture the so called quick flow and slow flow components [22]. Using this approach, more recent studies have shown improvements in streamflow forecasting by combining multiple models or generating ensemble estimates [5, 11, 12]. Such models can be used to systematically incorporate streamflow predictions into water control.

Automatic control has been widely applied to the regulation of water networks. Regulation of water levels in open canals for irrigation has a long history [8,20,27, 33,41]. Regulation of flows in urban water supply networks has focused on avoiding overflows from the sewerage into the supply network [26,31]. River systems present a much more complex set of objectives. Automatic control has been applied to problems in river navigation [34], hydro power generation [10], and water quality management [18, 19]. It has also been applied extensively to flood management [3,4,6,7, 13,14,24,32].

Model Predictive Control (MPC) is rapidly emerging as the method of choice for the design of automatic controllers. The benefits of MPC are, its ability to incorporate external disturbances to the system model and the convenience of applying constraints. With regards to flood control, disturbances are the inflows into the river network. In [4], a discrete time non linear model is used to model the river system considering the gate movement as well. This model is capable of capturing the non linear flow characteristics during a flood event. Simulations are used to show that MPC applied on this model is suitable for controlling floods in Demer river in Belgium.

A common assumption in previous work is that inflows are known a-priori. It is likely however, that streamflow characteristics may change suddenly in response to unexpected rainfall or due to unmeasured variables such as existing soil moisture in the catchment. In contrast to [4] where disturbance is assumed to be known, [30] considers disturbance uncertainty. The authors propose a new algorithm based on Multiple Model Predictive Control (MMPC). A Monte-Carlo analysis is carried out to generate an ensemble of predictions of the inflow. This results in a range of inflow scenarios and their probabilities. These scenarios correspond to multiple models on which predictive control is applied with a-priori probabilities acting as weighting factors. For instance, disturbance scenarios of three severity levels are considered. The probability of occurrence of these scenarios is estimated by using the ensemble of predictions. The risk of flooding is minimized by optimizing the outflow considering all of the disturbance models. Optimization is carried out by taking an ensemble average of individual cost functions derived for each of the models.

Inflow uncertainty is also addressed in [23] to develop an MPC framework for flood management, and evaluated on data collected at the Wivenhoe reservoir during the 2011 Queensland floods in Australia. In this paper, the set of all possible disturbances are considered where each inflow condition of the set is assumed to have the same probability. These disturbance conditions are formulated as a set of constraints and are applied to the MPC system. Robust control action for the reservoir outflow is calculated such that the system constraints also are not violated.

An alternative approach to handling uncertain disturbances was presented in [2] and is denoted Multiple Model Adaptive Control (MMAC). In this approach, a bank of multiple models is derived based on multiple disturbance scenarios. However a-priori values of probabilities are not available or assumed. Individual controllers are applied to each model. At the same time, measurements from the system output are fed to a bank of Kalman filters which correspond to the bank of models. The Kalman filter residuals are used to weight the corresponding MPC controller outputs.

This paper investigates the thesis that knowledge of the most likely inflow characteristic can improve the performance of a flood control strategy. It takes the approach in [2] and uses the Kalman filter to dynamically estimate the inflow that is most likely in a minimum mean square error sense. The main difference from [2] is that, this paper considers future disturbances. In order to optimize the control here we apply MPC. Therefore we call our method Adaptive Multi Model Predictive Control (AMMPC).

The performance of our AMMPC methodology is first evaluated using simulated data. The results show a significant improvement over the approach in [30]. It is also evaluated using field data from the 2011 Queensland floods and compared against [23]. The results demonstrate a significant improvement in performance over the scheme suggested by operational manual of Wivenhoe reservoir [35]. It has obtained a 32% lower peak volume level compared to the results in [23] while maintaining the same peak outflow level. According to [36], flood water has to be emptied from reservoir within 7 days after a major event. AMMPC method is shown to release 99% of the excess flood volume by the end of the major event while less amount of water is released by the method in [23].

The remainder of this paper is organized as follows. Problem formulation is carried out in Section 2 and Section 3 covers the methodology. Section 4 outlines numerical results where the benefits of our AMMPC method are demonstrated. Section 5 concludes the paper with a short discussion of results.

2 Problem Formulation

As stated in typical river operation manuals [21, 36], the objective of flood control is to minimize the likelihood of downstream river bank overflows by using reservoirs as buffers. River operators must also avoid overfilling or depleting storage reservoirs. Figure 1 is a schematic representation of a simplified river network consisting of two storage reservoirs and two inflows. The reservoirs are equipped with flow regulation devices (gates). The reservoir water levels are denoted by h_1 and h_2 with units of meters above a common reference point (e.g. mean sea level). The controlled outflow

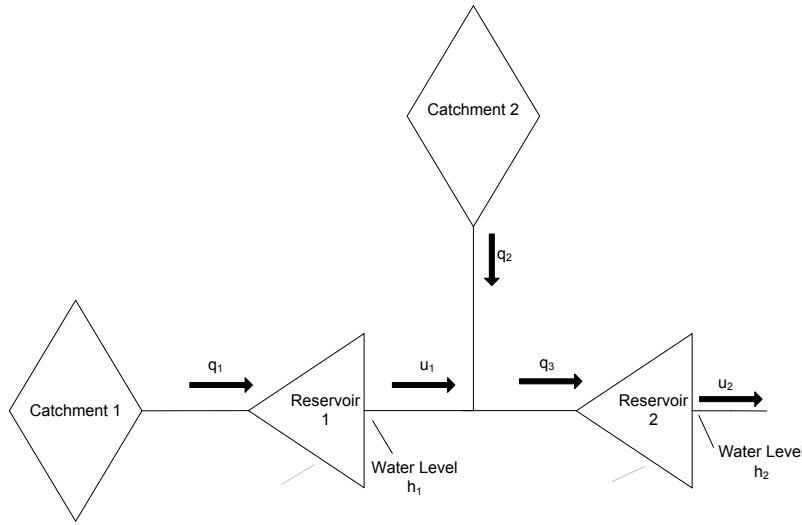


Fig. 1 Structure of a typical regulated river system: q_1 and q_2 are the inflows, u_1 and u_2 are the controlled outflows, h_1 and h_2 are the water levels (measured at downstream end) of the Reservoir 1 and Reservoir 2, respectively. There are no overflows under the controlled optimal outflows. ($q_3 = u_1 + q_2$)

or discharge from reservoirs 1 and 2 are denoted by u_1 and u_2 , respectively, and have units m^3/min . The inflow into Reservoir 1 is denoted by q_1 in m^3/min . The inflow into Reservoir 2 is the sum of the outflow from Reservoir 1 (u_1), and the inflow q_2 , also having units m^3/min . Variables used throughout this paper are listed in Table 1.

Main concern of this paper is real time flood management when there is uncertainty in the inflows q_1 and q_2 . If one has complete a-priori knowledge of these flows then it is possible to compute the controls u_1 and u_2 using optimal control theory [4]. In practice however, there can be a significant uncertainty in q_1 and q_2 due to spatial and temporal variations in expected rainfall and existing soil moisture levels across the catchment.

2.1 System Model

The first step is to adopt a modeling methodology for the river dynamics. The model must accurately reproduce the system dynamics for given inputs (e.g. inflows). In this case, the dynamics of interest include water levels and flow rates at key points of interest in the system. The most accurate approach is based on finite elements models that are derived using the river's underlying hydro dynamic principles. An example of this approach is the use of the Saint Venant hydrodynamic equations for

Table 1 Nomenclature

Symbol	Definition	Units
k	Time step index	–
T_c	Sampling time	<i>min</i>
A_s	Area of reservoir	m^2
h_1, h_2, h_1^*, h_2^*	Present/ target water levels in Reservoir 1 and 2	m
q_1, q_2, u_1, u_2	Inflows/ outflows of Reservoir 1 and 2	m^3/min
α_1, α_2	Balancing constants between flows and water levels for Reservoir 1 and 2	min/m^2
n_1, n_2	Time delays as multiples of T_c	–
β, τ, α	Impact/ time delay/ decay-rate of streamflow	$m^2/min, min, m^3/min^2$
i	Band index of catchment	–
r_i	Rain over i^{th} band	mm
w, v	Process/ measurement noise	m
Q_k, P_k	Variance of process/ measurement noise	m^2
\mathbf{x}_m	State of combined model	–
u	Manipulated input	m^3/min
y	Output	–
$\mathbf{A}_m, \mathbf{B}_m, \mathbf{C}_m, \mathbf{B}_d$	Characteristic matrices of state space and augmented state space models	–
$\mathbf{A}, \mathbf{B}, \mathbf{C}, \mathbf{R}$		–
\mathbf{x}	Augmented state	–
N, N_c	Prediction/ control horizon	<i>min</i>
$\Delta \mathbf{r}_c, \Delta \mathbf{u}_c$	Change of precipitation forecasts/ manipulated input over control horizon	$mm, m^3/min$
\mathbf{y}_c	Output states over control horizon	–
$\Delta \mathbf{r}, \Delta \mathbf{u}$	Change of precipitation forecasts/ manipulated input over one sample time	$mm, m^3/min$
$\Delta \mathbf{x}_m$	Change of state over one sample time	m
\mathbf{r}_s	Target state	–
$\Phi_1, \Phi_2, \mathbf{F}$	Matrices predicting states/ inputs/ outputs over control horizon	–
J	Cost function	–
$\mathbf{W}_s, \bar{\mathbf{R}}$	Output/ input weights	–
ψ_1, ψ_2, v_1, v_2	Outflow/ change of outflow constraints	m^3/min
p_i	Probability of i^{th} model being the actual model	–
$\mathbf{e}_i, \mathbf{S}_i$	Residual vector/ covariance matrix of i^{th} model	m, m^2
v, v_{FSC}	Volume/ Full supply capacity of Wivenhoe	m^3
\mathbf{q}, \bar{q}	Actual/ most likely inflow into Wivenhoe	m^3/s
\mathbf{d}_{in}	Uncertainty vector of inflows	m^3/s
\bar{q}_{rain}	Streamflow prediction with precipitation forecasts	m^3/s
\bar{q}_{som}	Inflow due to release from Somerset	m^3/s

modeling flows in open canals [1,9]. There are many software tools associated with this approach e.g. MOUSE, SIMBA, SIPSON, HYDROWORKS, KANSIM [26].

The alternative is the so called gray box approach which is loosely based on physical principles but largely rely on linear time invariant models validated using system identification principles [29]. This approach has been successfully used to develop models for open canals [40,41], river systems [15–17] and sewer networks [26]. Since most mathematically tractable and practical controller design strategies rely on linear time invariant models [26,28,41], we closely follow the gray box approach presented in [26,30,34] to model the river dynamics.

The starting point for the model is the conservation of volume and flow. For the water level h in a reservoir, this can be expressed as

$$\frac{dh}{dt} = \alpha[q_{in}(t - \delta) - q_{out}(t)] \quad (1)$$

where q_{in} is the inflow, q_{out} is the outflow and α is a constant of proportionality. The transport delay δ , appears in (1) because the water level h is presumed to be measured at the downstream end of the reservoir. For a river reach section we have the following simple model which gives the downstream flow q_d by,

$$q_d(t) = q_u(t - \delta) \quad (2)$$

where q_u is the upstream flow and here again δ is a transport delay from upstream to downstream.

It is important to note that (1) and (2) are linear models. However, it is well known that in flood conditions, natural river systems can exhibit non-linear dynamics. For example, the transport delay in (2) may be a function of flow rate. One way to handle this is to use non linear models. This may require non linear controller design. An alternative approach is to approximate the range of system dynamics by a bank of linear models. In this case, the control strategy may involve switching between the models. This paper does not address this issue and focuses instead on the additional challenge of uncertain disturbances. Future work will address the issue of non linear dynamics.

We shall be designing a discrete time controller and this requires a discrete time model. The following simple Euler approximation can be used to approximate the derivative in equation (1) :

$$\frac{dh}{dt} \approx \frac{h(T_c(k+1)) - h(T_c(k))}{T_c} \quad (3)$$

where T_c is the sample period and k is the time step index. From (1) and (3) the water level h_1 in Reservoir 1 is given by

$$h_1(k+1) = h_1(k) + \alpha_1(-u_1(k) + q_1(k - n_1)) \quad (4)$$

where $n_1 = \delta_1/T_c$ and δ_1 is the time delay for q_1 's effect to appear as a change in h_1 which is measured at the downstream end of the reservoir. By using (2), the flow rate q_3 into Reservoir 2 is given by

$$q_3(k) = u_1(k - n_4) + q_2(k - n_4) \quad (5)$$

where $n_4 = \delta_2/T_c$ and δ_2 is the transport delay along the river reach. Both the flows are measured at the same spot. By combining (3), (4) and (5) the water level h_2 in Reservoir 2 is given by

$$\begin{aligned} h_2(k+1) &= h_2(k) + a_2(q_3(k - n_3) - u_2(k)) \\ &= h_2(k) + \alpha_2(u_1(k - n_2) + q_2(k - n_2) - u_2(k)) \end{aligned} \quad (6)$$

where $n_2 = n_3 + n_4$. In equations (4) and (6), q_1 and q_2 are hereafter denoted as disturbances and u_1 and u_2 are denoted as controls to be calculated.

The first order linear time invariant models derived here, have been systematically applied to control design for irrigation canals. The key challenge is identifying the coefficients α_i and the transport delays n_i . The work in [29,40] employs system identification theory to solve this problem. As indicated before, linear time invariant

models do not capture all the system dynamics. However, linear higher order models or multiple model approach can be applied. In this paper we do not solve the identification problem and simply assume parameter values. In the case of the numerical results on the Wivenhoe dam, we use system model parameters presented in [23].

2.2 State Space Model

Armed with the models in equations (4) and (6) the next step is to develop a state space representation of the system dynamics [4]. The state space formulation makes it easier to handle the transport delays, and is required for the MMPC approach used here. We start this derivation by introducing the state variables

$$s_1(k) \triangleq h_1(k) \quad \text{and} \quad s_2(k) \triangleq h_2(k).$$

We also introduce state variables to store current and past value of the variables $q_1(k)$, $q_2(k)$ and $u_1(k)$ such that,

$$\begin{aligned} s_{i1}(k) &\triangleq q_i(k-1) \quad i=1,2 \\ s_{i2}(k) &= s_{i1}(k-1) = q_i(k-2) \\ &\vdots \\ s_{iN}(k) &= s_{iN-1}(k-1) = q_i(k-N) \end{aligned}$$

$$\begin{aligned} t_{i1}(k) &\triangleq u_i(k-1) \quad i=1 \\ t_{i2}(k) &= t_{i1}(k-1) = u_i(k-2) \\ &\vdots \\ t_{iN}(k) &= t_{iN-1}(k-1) = u_i(k-N). \end{aligned}$$

In this paper, symbols with bold capital letters represent matrices and values within subscripted parentheses show their sizes. Bold simple letters represent vectors. A new state vector $\mathbf{x}(k)$ is defined as

$$\mathbf{x}(k) = [s_1(k) \quad s_{11}(k) \quad \cdots \quad s_{1n_1}(k) \quad s_2(k) \quad s_{21}(k) \quad \cdots \quad s_{2n_2}(k) \quad t_{11}(k) \quad \cdots \quad t_{1n_2}(k)]^T$$

We can now express (4) and (6) in a state space form as

$$\mathbf{x}(k+1) = \mathbf{A}_m \mathbf{x}(k) + \mathbf{B}_m \mathbf{u}(k) + \mathbf{B}_q \mathbf{q}(k)$$

where $\mathbf{q}(k) = [q_1(k) \quad q_2(k)]^T$ and $\mathbf{u}(k) = [u_1(k) \quad u_2(k)]^T$. Values of $\mathbf{q}(k)$, $k = 1 \cdots N_c$ can be either known or a source of inflows such as a streamflow model will update their values. Tedious but straightforward manipulation results in

$$\mathbf{A}_m = \begin{bmatrix} \mathbf{A}_{1(n_1+1 \times n_1+1)} & \vdots & \mathbf{0}_{(n_1+1 \times 2n_2+1)} \\ \cdots & \cdots & \cdots \\ \mathbf{0}_{1(2n_2+1 \times n_1+1)} & \vdots & \mathbf{B}_{1(2n_2+1 \times 2n_2+1)} \end{bmatrix}$$

where

$$\mathbf{A}_1 = \begin{bmatrix} 1 & 0 & 0 & \cdots & 0 & 0 & \alpha_1 \\ 0 & 0 & 0 & \cdots & 0 & 0 & 0 \\ 0 & 1 & 0 & \cdots & 0 & 0 & 0 \\ 0 & 0 & 1 & \cdots & 0 & 0 & 0 \\ \vdots & \vdots & \vdots & \ddots & \vdots & \vdots & \vdots \\ 0 & 0 & 0 & \cdots & 1 & 0 & 0 \\ 0 & 0 & 0 & \cdots & 0 & 1 & 0 \end{bmatrix}$$

$$\mathbf{B}_1 = \begin{bmatrix} 1 & 0 & \cdots & 0 & \alpha_2 & 0 & \cdots & 0 & 0 & \alpha_2 \\ 0 & 0 & \cdots & 0 & 0 & 0 & \cdots & 0 & 0 & 0 \\ 0 & 1 & \cdots & 0 & 0 & 0 & \cdots & 0 & 0 & 0 \\ 0 & 0 & \cdots & 1 & 0 & 0 & \cdots & 0 & 0 & 0 \\ \vdots & \vdots & \ddots & \vdots & \vdots & \vdots & \ddots & \vdots & \vdots & \vdots \\ 0 & 0 & \cdots & 0 & 0 & 0 & \cdots & 1 & 0 & 0 \\ 0 & 0 & \cdots & 0 & 0 & 0 & \cdots & 0 & 1 & 0 \end{bmatrix}$$

$$\mathbf{B}_m = \begin{bmatrix} -\alpha_1 & 0 & \cdots & 0 & \vdots & 0 & \cdots & 1 & \cdots & 0 \\ 0 & 0 & \cdots & 0 & \vdots & -\alpha_2 & \cdots & 0 & \cdots & 0 \end{bmatrix}^T$$

and

$$\mathbf{B}_q = \begin{bmatrix} 0 & 1 & \cdots & 0 & \vdots & 0 & 0 & \cdots & 0 \\ 0 & 0 & \cdots & 0 & \vdots & 0 & 1 & \cdots & 0 \end{bmatrix}^T.$$

To account for modeling errors we introduce a process noise term $\mathbf{w}(k) \sim \mathcal{N}(0, Q_k)$ normally distributed with zero mean and variance Q_k so that we have

$$\mathbf{x}_m(k+1) = \mathbf{A}_m \mathbf{x}_m(k) + \mathbf{B}_m \mathbf{u}(k) + \mathbf{B}_q \mathbf{q}(k) + \mathbf{w}(k). \quad (7)$$

It is assumed that all state variables are available and we have the accompanying state observation vector $\mathbf{y}(k)$

$$\mathbf{y}(k) = \mathbf{C}_m \mathbf{x}_m(k) + \mathbf{v}(k) \quad (8)$$

where \mathbf{C}_m a diagonal matrix with '1's at the places corresponding to $h_1(k)$ and $h_2(k)$ to exclude the effect of other state variables except water levels. Thus $\mathbf{y}(k)$ takes the form,

$$\mathbf{y}_m(k) = [h_1(k) \quad 0 \quad \cdots \quad h_2(k) \quad 0 \quad \cdots] ^T.$$

Measurement noise is normally distributed with zero mean and variance P_k i.e. $\mathbf{v}(k) \sim \mathcal{N}(0, P_k)$ and is intended to capture measurement errors.

3 Methodology

The main contribution of this paper is the AMMPC automatic controller. The algorithm is outlined in Fig. 2. The approach involves a bank of independent MPC controllers and Kalman filters. A set of disturbances are used to build the corresponding set of state space models. Each Model Predictive Controller calculates the control $\mathbf{u}_i(k)$. The accompanying Kalman filter predicts the system state at each time step. The controller outputs are combined using a measure of the likelihood of each model's validity as calculated by the Kalman filter's innovation covariance. This combined control output is applied to the system. Convergence characteristics of the Kalman filter weights is to be investigated in a future publication. However simulated results show convergence in general.

3.1 MPC Algorithm

Model predictive control is widely used in process control systems. It is easy to incorporate system constraints using MPC, and it also allows for state space formulation which is essential in a multi variable framework, and when incorporating time delays.

The general form of state space models can be given by (7) and (8). There are different ways of formulating the MPC problem using the state space model. A method called Non Minimal State Space approach [38,39] is used here. It has added advantages in MPC. Firstly, it avoids using a state observer to estimate the state of the system which can cause problems when handling constraints. It also reduces steady state error. According to this approach the augmented state space model is formulated from the above state space model given by equations (7) and (8) as

$$\begin{aligned}\mathbf{x}(k+1) &= \mathbf{A}\mathbf{x}(k) + \mathbf{B}\Delta\mathbf{u}(k) + \mathbf{Q}\Delta\mathbf{q}(k) + \mathbf{W}\Delta\mathbf{w}(k) + \mathbf{V}\mathbf{v}(k+1) \\ \mathbf{y}(k) &= \mathbf{C}\mathbf{x}(k)\end{aligned}$$

where

$$\Delta\mathbf{x}(k) = \mathbf{x}(k) - \mathbf{x}(k-1)$$

$$\mathbf{x}(k) = \begin{bmatrix} \Delta\mathbf{x}_m(k) \\ \mathbf{y}(k) \end{bmatrix}$$

$$\mathbf{A} = \begin{bmatrix} \mathbf{A}_m & \mathbf{0} \\ \mathbf{C}_m\mathbf{A}_m & \mathbf{I} \end{bmatrix}$$

$$\mathbf{B} = \begin{bmatrix} \mathbf{B}_m \\ \mathbf{C}_m\mathbf{B}_m \end{bmatrix}$$

$$\Delta\mathbf{u}(k) = \mathbf{u}(k) - \mathbf{u}(k-1)$$

$$\mathbf{Q} = \begin{bmatrix} \mathbf{B}_q \\ \mathbf{C}_m\mathbf{B}_q \end{bmatrix}$$

$$\Delta \mathbf{q}(k) = \mathbf{q}(k) - \mathbf{q}(k-1)$$

$$\mathbf{W} = \begin{bmatrix} \mathbf{I} \\ \mathbf{C}_m \end{bmatrix}$$

$$\Delta \mathbf{w}(k) = \mathbf{w}(k) - \mathbf{w}(k-1)$$

$$\mathbf{V} = \begin{bmatrix} \mathbf{0} \\ \mathbf{I} \end{bmatrix}$$

and

$$\mathbf{C} = [\mathbf{0}_m \mathbf{C}_m].$$

Let N be the prediction horizon and N_c be the control horizon. The future values of the model parameters along the prediction window are made to propagate using the method of substitution (refer [38] for details). Define

$$\mathbf{x}_c \triangleq [\mathbf{x}(k+1/k) \quad \mathbf{x}(k+2/k) \quad \cdots \quad \mathbf{x}(k+N/k)]^T,$$

$$\Delta \mathbf{u}_c \triangleq [\Delta \mathbf{u}(k) \quad \Delta \mathbf{u}(k+1) \quad \cdots \quad \Delta \mathbf{u}(k+N_c-1)]^T,$$

$$\Delta \mathbf{q}_c \triangleq [\Delta \mathbf{q}(k) \quad \Delta \mathbf{q}(k+1) \quad \cdots \quad \Delta \mathbf{q}(k+N_c-1)]^T.$$

Now the set of propagated system parameters can be concatenated as

$$\mathbf{x}_c = \mathbf{F}\mathbf{x}(k) + \phi_1 \Delta \mathbf{u}_c + \phi_2 \Delta \mathbf{q}_c$$

where

$$\mathbf{F} = [\mathbf{A} \quad \mathbf{A}^2 \quad \cdots \quad \mathbf{A}^N]^T$$

$$\phi_1 = \begin{bmatrix} \mathbf{B} & \cdots & \cdots & \cdots & \mathbf{0} \\ \mathbf{AB} & \mathbf{B} & \cdots & \cdots & \mathbf{0} \\ \vdots & \vdots & \vdots & \ddots & \vdots \\ \mathbf{A}^{N-1}\mathbf{B} & \mathbf{A}^{N-2}\mathbf{B} & \mathbf{A}^{N-3}\mathbf{B} & \cdots & \mathbf{A}^{N-N_c}\mathbf{B} \end{bmatrix}$$

with an analogous form for $\phi_2(\mathbf{A}, \mathbf{Q})$. Armed with the above, we define the linear quadratic MPC criterion for set point tracking,

$$\begin{aligned} \text{minimize} \quad & [\mathbf{r}_s - \mathbf{x}_c]^T \mathbf{W}_s [\mathbf{r}_s - \mathbf{x}_c] + \Delta \mathbf{u}_c^T \bar{\mathbf{R}} \Delta \mathbf{u}_c + \sum_{k=1}^{N_c} \mathbf{c} \mathbf{e} \\ \text{subject to} \quad & 0 \leq \mathbf{u}(k) \leq \psi, \\ & \Delta \mathbf{u}(k) \leq v. \end{aligned} \tag{9}$$

where r_s is the system target state, ψ and v are the maximum limits imposed on the respective variable, \mathbf{e} is a slack variable, \mathbf{c} is its penalty value, \mathbf{W}_s and $\bar{\mathbf{R}}$ are the weighing matrices. Here, \mathbf{W}_s has '1's at the places corresponding to $h_1(k)$ and $h_2(k)$ to

exclude the effect of other state variables except the water levels. The matrix \mathbf{W}_s has dimensions $[\dim(\mathbf{x}(k)) \times N]$ and the matrix $\bar{\mathbf{R}}$ has dimensions $[\dim(\mathbf{u}(k)) \times N]$ where \dim denotes dimensions. They are used to trade-off control effort and set point tracking response times. The summation term is applied only when the problem consists of soft constraints which can be violated at worse case scenarios. The slack variable \mathbf{e} is a vector which represents the maximum violation of each of these constraints. Violating these constraints is penalized by the vector \mathbf{c} . However in this simple case we do not consider soft constraints. Given h_1^* and h_2^* are the target water levels of the reservoirs, system target state is

$$\mathbf{r}_s = [h_1^* \ 0 \ \dots \ 0 \ h_2^* \ 0 \ \dots \ 0]^T.$$

The two hard constraints mentioned in the cost function minimization can be described as follows. In order to avoid hazards, water should be released from the gates in a controlled manner. Outflows of high scale as well as sudden flow changes of high intensity can cause negative impacts on the infrastructure. When $\mathbf{u}(k)$ is the optimal outflow at the k^{th} time, the constraints on the system become,

$$0 \leq \mathbf{u}(k) \leq \boldsymbol{\psi}$$

and

$$\Delta \mathbf{u}(k) \leq \mathbf{v}.$$

The MPC constrained optimization problem in (9) is solved using the Hildreth quadratic programming [38]. According to this procedure, the cost function is taken as the primal problem and the Hildreth procedure gives the solution to its dual problem. This yields the sequence of increments upon the outflows for a period of N_c , represented by $\Delta \mathbf{u}_c$ where $\Delta \mathbf{u}_c = [\Delta \mathbf{u}(k), \dots, \Delta \mathbf{u}(k + N_c)]$.

Given that,

$$\mathbf{u}_c(k) = [\mathbf{u}(k) \ \mathbf{u}(k+1) \ \mathbf{u}(k+2) \ \dots \ \mathbf{u}(k+N_c)]$$

where $\mathbf{u}(k), \dots, \mathbf{u}(k+N_c)$ are the optimal outflows to be applied at the time steps $k \dots k+N_c$, it is possible to calculate $\mathbf{u}_c(k)$ by using the relationship

$$\mathbf{u}_c(k) = \mathbf{u}_c(k-1) + \Delta \mathbf{u}_c.$$

3.2 Kalman Filter Algorithm

The Kalman filter is used to estimate the system state such that the mean square prediction error is minimised. The Kalman filter has two stages: prediction and update. For the system given in (7) and (8), the prediction and update stages are given in the Table 2. Prediction is based on iterating the state equations. Once the measurement $y(k)$ is received the update of the state estimate takes place based upon the measurement residual.

Under ideal conditions, the steady state mean prediction error should converge to zero. In the case of model mismatch we expect to see non-zero mean prediction error. This error can be used as a measure of disturbance model's accuracy. AMMPC

Table 2 Kalman Filter Algorithm

Prediction Stage	
Predicted state estimate	$\hat{\mathbf{x}}_{k/k+1} = \mathbf{A}_m \hat{\mathbf{x}}_{k-1/k-1} + \mathbf{B}_m \mathbf{u}(k) + \mathbf{B}_q \mathbf{q}(k)$
Predicted estimate covariance	$\mathbf{P}_{k/k+1} = \mathbf{A}_m \mathbf{P}_{k/k-1} \mathbf{A}_m^T + \mathbf{Q}_k$
Innovation or measurement residual	$\mathbf{e}(k) = \mathbf{y}(k) - \mathbf{A}_m \hat{\mathbf{x}}_{k/k+1}$
Innovation covariance	$\mathbf{S}(k) = \mathbf{C}_m \mathbf{P}_{k/k+1} \mathbf{C}_m^T + \mathbf{R}_k$
Optimal Kalman gain	$\mathbf{K}(k) = \mathbf{P}_{k/k+1} \mathbf{C}_m^T \mathbf{S}(k)^{-1}$
Updated state estimate	$\hat{\mathbf{x}}_{k/k} = \hat{\mathbf{x}}_{k/k-1} + \mathbf{K}(k) \mathbf{e}(k)$
Updated estimate covariance	$\mathbf{P}_{k/k} = (\mathbf{I} - \mathbf{K}(k) \mathbf{C}_m) \mathbf{P}_{k/k+1}$

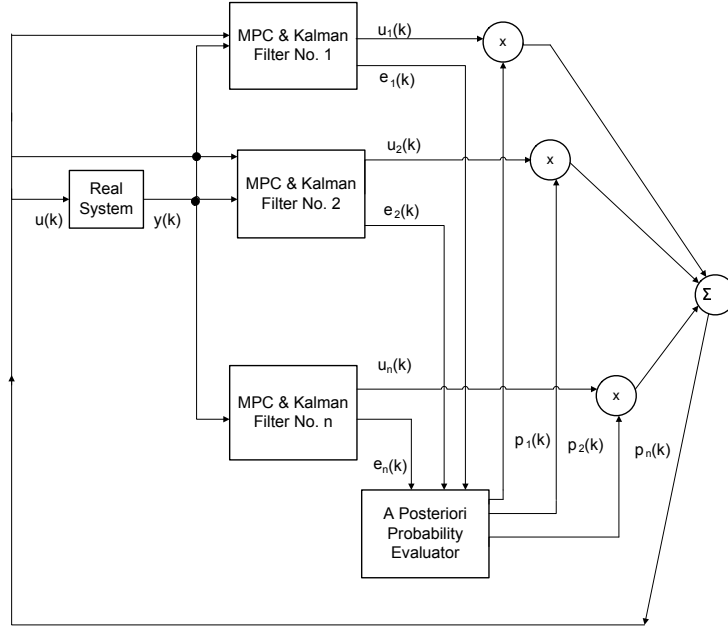


Fig. 2 Extended version of the structure of a typical MMPC system as in [2]. Each Model Predictive Controller (MPC) i calculates the optimal control $u_i(k)$ according to its model parameters. Actual control applied on the real system $u(k)$ is the weighted sum of all the optimal controls thus calculated. Each weight p_i is calculated by i^{th} Kalman filter based on the residuals $e_i(k)$ of the measurements $y(k)$

approach exploits this to calculate a new control vector as a weighted sum of the individual control vectors.

Procedure for AMMPC as given in [2] follows: The conditional density function of the measurement $\mathbf{y}(k)$ for the i^{th} Kalman filter, conditioned on the measurement history $\mathbf{Y}(k-1) = [\mathbf{y}(1) \ \mathbf{y}(2) \ \dots \ \mathbf{y}(k-1)]$ and a given hypothesis H_i (i.e. a disturbance event out of the set of disturbances) is given by

$$f(\mathbf{y}(k)/H_i, \mathbf{Y}(k-1)) = \rho_i^* \exp(m_i(k))$$

where

$$\rho_i^* = [(2\pi)^{N'} \det \mathbf{S}_i]^{-1/2}, \quad i = 1, 2, \dots, n.$$

Here, \exp is the exponential, N' is the number of state variables, n is the number of models in the bank and S_i is the residual covariance matrix of the i^{th} Kalman filter (refer to Table 2), whereas

$$m_i(k) = -\frac{1}{2} \mathbf{e}_i(k)^T \mathbf{S}_i^{-1} \mathbf{e}_i(k)$$

where $e_i(k)$ is the residual vector given in Table 2. Conditional probability for a particular hypothesis posteriori to the measurements is given by

$$\begin{aligned} p_i(k) &= Pr(H = H_i | Y(k) = y(k)) \\ &= \frac{f(y(k)/H_i, Y(k-1)) \cdot p_i(k-1)}{\sum_{j=1}^n f(y(k)/H_j, Y(k-1)) \cdot p_j(k-1)}. \end{aligned}$$

Then, the probability $p_i(k)$ for each model i becomes,

$$p_i(k) = \frac{p_i(k-1) \rho_i^* \exp[m_i(k)]}{\sum_{j=1}^n p_j(k-1) \rho_j^* \exp[m_j(k)]}.$$

In this equation we use the prior conditional probabilities, $p_i(k)$ to weight the conditional densities of the current measurements, assuming each hypothesis, and then normalize it over the complete set of numerator terms. For failure identification applications, where we usually want to choose the most likely hypothesis out of the set of possible hypotheses, we can choose the hypothesis with the largest conditional probability. This procedure happens subsequently to the measurements. Hence, the evaluation of probabilities is a posteriori measure, originating the name ‘‘A-posteriori Probability Evaluator’’ in Fig. 2. Another explanation is that S_i measures the a-posteriori mean square error of a measurement. Therefore $p_i(k)$ is a measure of the probability of Model i to have the minimum mean square error compared to other models. When the error is higher, $p_i(k)$ gets smaller. Finally, the control $\mathbf{u}(k)$ becomes

$$\mathbf{u}(k) = \sum_{i=1}^n p_i(k) \mathbf{u}_i(k).$$

To find the disturbance model bank, experimental statistics can be used.

4 Numerical Results

In this section we evaluate the performance of our solution using two methods. In the first method we use a simulation model to demonstrate the performance of our solution. In the second method, we use data measured at the Wivenhoe dam during the 2011 Queensland floods in Australia. Simulations are implemented using Matlab R2010a. The simulation parameters are listed in Table 3.

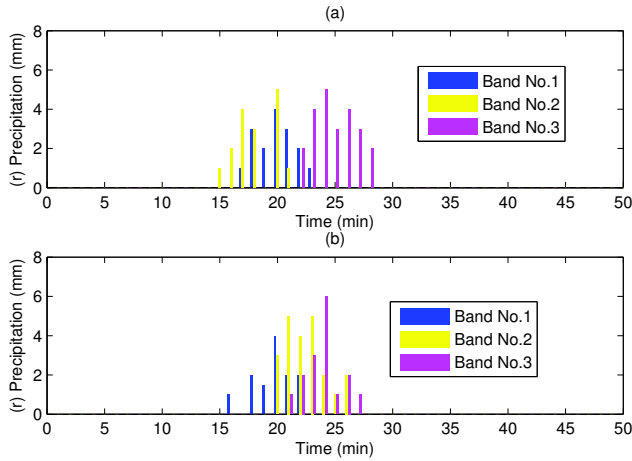


Fig. 3 Precipitation across (a) Catchment No.1 (b) Catchment No.2

Method 1: Simulated River Network and Inflows

Figure 1 is the schematic illustration of the model used in this simulation study. Streamflow is simulated based on the model in [25] and is described in further detail in the following paragraph. We compare our AMMPC approach with that presented in [30].

Streamflow Model

The catchment under consideration is divided by equi-height contour lines into one or more elevation bands. Total resultant streamflow is a linear accumulation of the rainfall in each band. The combined streamflow in the basin $q(k)$ becomes

$$q(k) = \sum_{i=1}^b \sum_{j=0}^{k-\tau(i)} (k-j-\tau(i))\beta(i)e^{-\frac{k-j-\tau(i)}{\alpha(i)}} r_i(j) \quad (10)$$

where i is the index of the band, b is the number of bands, r_i is the rainfall across the i^{th} band, $\beta(i)$ is the relative importance (weighting) of the band, $\tau(i)$ is the time delay between the rainfall event and the resulting increase in the streamflow and $\alpha(i)$ is the decay rate which is the rate at which the impact of a rainfall event on streamflow subsides. According to the model, any streamflow condition can be represented by the 3-tuple (τ, α, β) .

The following assumptions are made in the development of the test case. The sample interval $T_c = 1 \text{ min}$. In reality, this sample time could be in multiple minutes. There are two catchments. Each catchment area has three bands. There are no cross

Table 3 Parameters used in the simulations and their values

Symbol	Value	Units
n_1	3	—
n_2	5	—
h_1	50	m
h_2	20	m
h_1^*	50	m
h_2^*	20	m
\mathbf{Q}_k	0.001	m^2
\mathbf{P}_k	0.001	m^2
N	50	min
N_c	45	min
α_1	1	min/m^2
α_2	1	min/m^2
ψ_1	20	m^3/min
ψ_2	20	m^3/min
v_1	4	m^3/min
v_2	4	m^3/min
P_{min}	0.1	—
P_{avg}	0.8	—
P_{max}	0.1	—
\mathbf{R}	50 I_{90}	—

Table 4 Streamflow models and their parameters

Model No.	Band No.	Catchment 1	Catchment2
		(τ, α, β)	(τ, α, β)
1 (minimum inflow)	1	(2, 0.1, 0.5)	(1, 0.1, 1)
	2	(3, 0.2, 1)	(2, 0.2, 1.5)
	3	(4, 0.3, 1.5)	(6, 0.3, 2)
2 (average inflow)	1	(3, 0.3, 2.5)	(2, 0.3, 3)
	2	(2, 0.4, 3)	(1, 0.4, 3.5)
3 (maximum inflow)	3	(4, 0.5, 3.5)	(6, 0.5, 4)
	1	(4, 0.5, 4.5)	(6, 0.5, 5)
	2	(2, 0.6, 5)	(1, 0.6, 5.5)
	3	(3, 0.7, 5.5)	(2, 0.7, 6)

connections between individual catchments. Three streamflow models are defined in Table 4 corresponding to minimum, average and maximum inflows in order. The models are ranked by a “model number”. We also assume no overflow, and generate the inflow accordingly.

The state space model is developed for the system in Fig. 1 using the results in 2.2, where the inflows denoted by q in equations (7) and (8) are given by (10). For brevity, we omit restating the resultant equations.

Before presenting the simulation results, we outline an alternative approach presented in [30]. In this approach, the three disturbance scenarios are incorporated into the controller, a minimum inflow, a maximum inflow and an average inflow scenario. As a result, there are three state space models representing each of these inflow scenarios. P_{min} , P_{avg} and P_{max} are the probability of occurrence of minimum, average

and maximum scenarios, respectively. In practice, these probabilities are based on statistics of past meteorological observations. The total risk to the system is defined as the product of the probability of occurrence of an inflow scenario and the resultant deviation from control set points which are water levels in this case. The cost function in [30] takes the form of

$$J = P_{min} l_{min}^2 + P_{avg} l_{avg}^2 + P_{max} l_{max}^2 + \Delta \mathbf{u}_c^2 \quad (11)$$

where l_{min} , l_{avg} and l_{max} are the deviations of water level from the target level during minimum, average and maximum scenarios, respectively. We use this cost function to compare against our AMMPC approach. To do this, the model given by equations (7) and (8) is substituted in (11), and the resulting minimization process is used as an alternative method for flood control. The cost function to be minimized becomes

$$J = P_{min} [\mathbf{r}_s - \mathbf{x}_{c(min)}]^T \mathbf{W}_s [\mathbf{r}_s - \mathbf{x}_{c(min)}] + P_{avg} [\mathbf{r}_s - \mathbf{x}_{c(avg)}]^T \mathbf{W}_s [\mathbf{r}_s - \mathbf{x}_{c(avg)}] \\ + P_{max} [\mathbf{r}_s - \mathbf{x}_{c(max)}]^T \mathbf{W}_s [\mathbf{r}_s - \mathbf{x}_{c(max)}] + \Delta \mathbf{u}_c^T \bar{\mathbf{R}} \Delta \mathbf{u}_c.$$

Recall that \mathbf{x}_c , \mathbf{r}_s , $\Delta \mathbf{u}_c$, \mathbf{W}_s and $\bar{\mathbf{R}}$ are defined in Section 2. Here, subscripts *min*, *avg* and *max* correspond to minimum, average and maximum scenarios, respectively. The constraints are as same as those applied with the cost function given by equation (9).

The initial and target water levels for Reservoir 1 are h_1 and h_1^* , respectively. Those for Reservoir 2 are h_2 and h_2^* , respectively. The parameters and their values are given in Table 3. Precipitation input is illustrated in Fig. 3. We assume that the inflows are generated from the data given in Table 4. According to the values in Table 4, P_{avg} is high. This implies that the model used in MMPC [30] has a high level of expectation for average inflow.

Figures 4 to 6 show how water levels respond to inflow variability in the minimum, average and maximum inflows under AMMPC and MMPC [30] methods. Results show that, under average inflow scenario both methods achieve water level set points. However, under minimum and maximum inflow scenarios only the AMMPC method is able to perform as in the average scenario. The water level set points are violated by MMPC [30] method.

The method based on [30] performs poorly because the a-priori probabilities are biased to a average flow scenario whereas our AMMPC approach adapts to the specific scenario. This results in a mismatch between the actual system model and the controller model in the MMPC [30] method. AMMPC method is able to identify the current inflow scenario based on current measurements and make the controller match with the actual model. The results presented in this section illustrate the advantage of taking inflow uncertainty and variability into consideration in the case of changing catchment characteristics.

Method 2: Real River Network and inflows

In this study, we evaluate our AMMPC approach using data collected at the Wivenhoe dam during the 2011 Queensland floods in Australia. The schematic diagram of the network is shown in Fig. 8. Wivenhoe reservoir is the main flood control

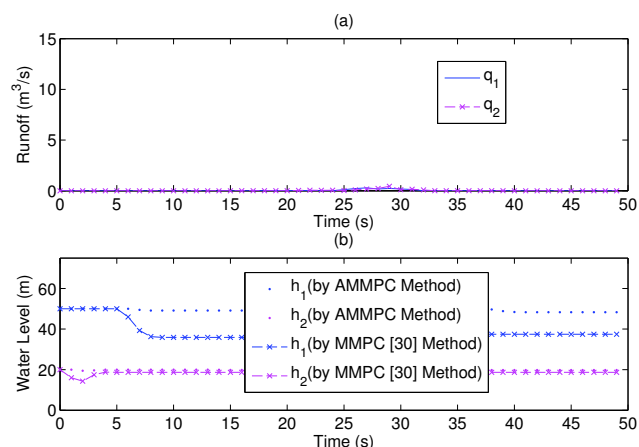


Fig. 4 (a) Minimum inflow (corresponding to Model No.1) entering the river system and (b) reservoir water levels resulted by AMMPC and MMPC [30] methods (q_1 and h_1 for Reservoir 1, q_2 and h_2 for Reservoir 2)

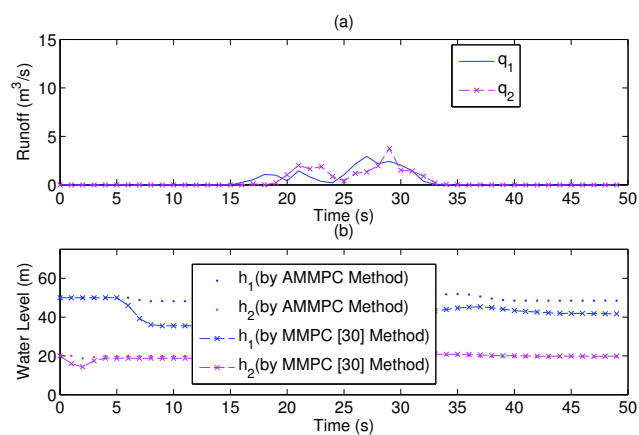


Fig. 5 (a) Average inflow (corresponding to Model No.1) entering the river system and (b) reservoir water levels resulted by AMMPC and MMPC [30] methods (q_1 and h_1 for Reservoir 1, q_2 and h_2 for Reservoir 2)

reservoir on the Brisbane river. It has a flood control volume of 1.45×10^6 ML as well as a Full Supply Capacity (FSC) of 1.65×10^6 ML for urban water needs.

Lowood and Moggill are two strategically important points further downstream 10 km and 50 km (approximately), respectively from Wivehoe dam. Flow measurements at these locations are used to estimate the existence and severity of flooding downstream the dam. The current control strategy for the dam consists of four phases which governs the outflow from the dam [36]. The first option is to maintain the flow at Lowood below $1900 m^3/s$. If this fails, the second and third options are to maintain the flow at Moggill firstly at $3500 m^3/s$ and then at $4000 m^3/s$. The final option is to

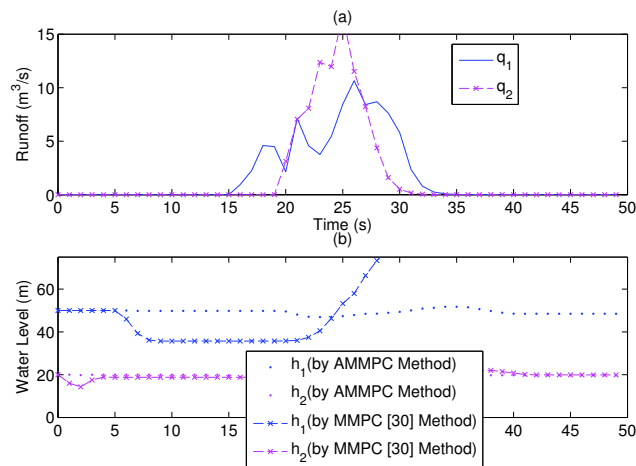


Fig. 6 (a) Maximum inflow (corresponding to Model No.1) entering the river system and (b) reservoir water levels resulted by AMMPC and MMPC [30] methods (q_1 and h_1 for Reservoir 1, q_2 and h_2 for Reservoir 2)

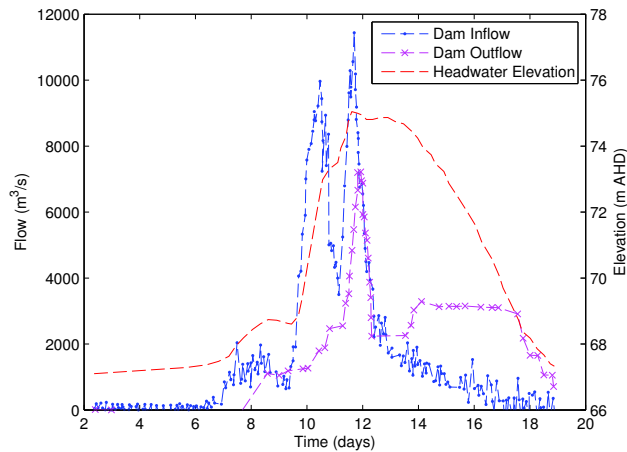


Fig. 7 Wivenhoe Dam inflow and release summary for the January 2011 Flood Event extracted from [35]. note: AHD = Australian Height Datum

avoid dam overflow at any cost e.g. by activating the fuse plugs for emergency release of water.

In the days leading up to 6th January 2011, there had been significant rainfall upstream of the dam which was already at the FSC. On 11th January, the dam operator made an emergency release in accordance to their procedure outlined above. It is clear from the data in [35] and Fig. 7, that the water release was initiated much too late. The outflow has responded to the inflow surge approximately 48 hours too late causing a high volume to build up in the dam. This highlights the importance of pre-release

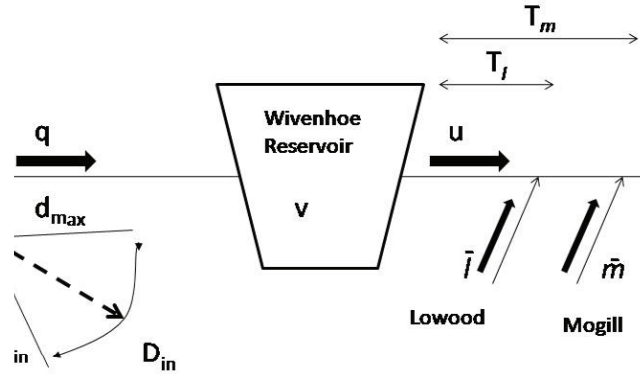


Fig. 8 Flows coming into and going out of Wivenhoe Dam where q is the total inflow, \bar{q} is the most likely inflow, \mathbf{d}_{in} is the uncertain inflow, q_{rain} is the inflow calculated with precipitation forecasts, q_{som} is the outflow from Somerset dam, v is the reservoir volume, u is the outflow, T_l and T_m are the times for the outflow to reach Lowood and Moggill and \bar{l} and \bar{m} are the flows at these locations along the prediction horizon. Uncertain inflow \mathbf{d}_{in} belongs in the range D_{in} .

of water in response to inflow forecasts. Under such a situation, predictive control provides a suitable framework to control outflows.

One such attempt is presented in [23] where the predicted inflows as well as their uncertainties are considered. The set of predicted inflows are considered where each inflow is assumed to have the same probability. This method achieves lower peak volume and outflow levels compared to those resulting from the reservoir operational manual.

We now outline our approach to this problem. We develop the system model based on Fig. 8, formulate the state space model and then add the constraints as discussed in Sections 2 and 3. The model parameters are obtained from [23]. As per Fig. 8, the volume of the reservoir v is given by,

$$v(k+1) = v(k) + \gamma[q(k) - u(k)] \quad (12)$$

where q is the inflow to the reservoir and u is the outflow from the reservoir. The constant $\gamma = 3.6$ converts flow in m^3/s to ML for a sample period $T_c = 1$ hour. The inflow q is calculated by,

$$\mathbf{q}(k) = \bar{q}(k) + \mathbf{d}_{in}(k) \text{ for } \mathbf{d}_{in}(k) \in D_{in}(k) \quad (13)$$

where \bar{q} is the most likely inflow predicted from the hydrological model URBS, d_{in} is the uncertain inflow and D_{in} is the associated inflow uncertainty set.

Figure 9 gives measured and predicted inflows into Wivenhoe reservoir [35]. The symbol ‘o’ indicates the start of a new prediction run. Predicted inflow trajectories for each of these runs are shown in different colors. A new prediction trajectory is created after a new prediction run is made and this trajectory is taken as \bar{q} . Then the previous trajectories are discarded. Around \bar{q} , set of \mathbf{d}_{in} values are selected as in (13) and they will build the multiple state space models. As mentioned in Section 3, value of q can either be known throughout the control horizon or updated time to time. Latter case is applied here and q is recalculated at each new prediction run. Most likely inflow \bar{q} is given by

$$\bar{q}(k) = q_{rain}(k) + q_{som}(k)$$

where q_{rain} is the predicted inflow considering precipitation forecasts and q_{som} is the outflow from Somerset reservoir up river the Wivenhoe.

The main difference between our method and that in [23] is that the uncertain inflows d_{in} are addressed in a different manner. In [23], different uncertain inflows d_{in} within D_{in} are formulated into a set of constraints. In our method, we define number of disturbance models to cover the full range of D_{in} . Multi state space models are built by incorporating the disturbance models to the system model given by (12) as in Section 2. Here it is assumed that there is a linear relationship to relate the reservoir volume to the water level which is the measureable variable. Finally, the state space models take the form of those given by (7) and (8). MMPC problem is formulated as in Section 3.

The actual inflow resembles one out of the given models during one short period. The calculation extends up to the point $k + N_c$ of the current inflow trajectory unless replaced by a trajectory resulting from a new run. When such is the case, a new disturbance model set is created around the new inflow scenario. Once the control is applied, its effect is compared with the measured inflow. The residuals are calculated and control is refined in order to match the actual inflow. We now define the constraints to the problem.

Flows at Lowood and Moggill excluding the Wivenhoe outflow throughout the prediction horizon are denoted by $\bar{\mathbf{I}}$ and $\bar{\mathbf{m}}$, respectively. Even though exact measurements are not available for these flows, it is assumed that the most recent prediction to be equal to actual or measured flows at Lowood and Moggill. Transport delays are T_l and T_m . As in [23] $T_l = 3 \text{ hr}$ and $T_m = 18 \text{ hr}$.

There is a constraint on the outflow from the reservoir which is the upper limit of $10000 \text{ m}^3/\text{s}$. The reservoir volume should not exceed $2.25 \times 10^6 \text{ ML}$ which is the fuse plug activation capacity, and the target is to maintain it at $1.165 \times 10^6 \text{ ML}$. There should be a rate of change constraint however, as in [23] that is not applied. So the hard constraints become

$$u(k) \leq 10000$$

and

$$x(k) \leq 2250000.$$

Six river sections along the river are selected and the discharges at these locations are formulated as soft constraints. For example, the flow at Lowood should be below $1900 \text{ m}^3/\text{s}$ and that at Moggill should be below $4000 \text{ m}^3/\text{s}$. The flows at these six river sections are listed with their upper limits as follows:

$$\begin{bmatrix} u(k) + \bar{\mathbf{1}}(k + T_l) \\ u(k) + \bar{\mathbf{1}}(k + T_l) \\ u(k) + \bar{\mathbf{1}}(k + T_l) \\ u(k) + \bar{\mathbf{1}}(k + T_l) \\ u(k) + \bar{\mathbf{1}}(k + T_l) \\ u(k) + \bar{\mathbf{m}}(k + T_m) \end{bmatrix} - e \leq \begin{bmatrix} 50 \\ 100 \\ 200 \\ 430 \\ 1900 \\ 4000 \end{bmatrix}$$

where e is a slack variable which represents the maximum violation of each of the imposed soft constraints. The penalties of violating the constraints are given by the vector \mathbf{c} . Its elements can be set according to the relative impact of flooding at the given river section. We have used the values given in [23].

With these requirements the cost function of bringing the water volume to target state while maintaining the soft constraints becomes,

$$J = [x_c - v_{FSC}]^T W_s [x_c - v_{FSC}] + \Delta u_c^T \bar{R} \Delta u_c + \sum_{k=1}^{N_c} c e$$

where v_{FSC} is the full supply capacity. The control horizon N_c for this problem is 48 hours. After adding the hard constraints on flow and volume, the optimization problem becomes

$$\begin{aligned} & \text{minimize} \quad [x_c - v_{FSC}]^T W_s [x_c - v_{FSC}] + \Delta u_c^T \bar{R} \Delta u_c + \sum_{k=1}^{N_c} c e \\ & \text{subject to} \quad 0 \leq u(k) \leq 10000 \\ & \quad \quad \quad x(k) \leq 2250000. \end{aligned}$$

In this paper it is also assumed that noise characteristics are known and are equal to those given in Table 3. Figure 10 gives the actual outflow and the resultant outflow by our AMMPC method. The reservoir volume is shown in Fig. 11. The resultant flows downriver at Moggill and Lowood are given in Fig. 12. It can be seen that the resultant peak outflow from Wivenhoe under AMMPC method is close to that in [23] (approximately $3300 \text{ m}^3/\text{s}$) and significantly lower than the measured outflow during the event. It is also notable that our AMMPC method releases water in advance of both the other schemes. As a result, the peak volume is 1.5×10^6 ML under AMMPC as opposed to 2.2×10^6 ML in other two methods. The simulation has to stop at the 185th hour due to that the data is not available. However, by this time 99% of the inflow volume would be removed. This is in agreement with the flood control strategy in [36] where the flood water should be released from the reservoir within 7 days after the major event. In contrast, the method in [23] releases only a small amount of water during the major event forcing it to release water at around $2000 \text{ m}^3/\text{s}$ continuously till the end of the 7th day. This will cause high flow levels in Lowood and Moggill. Under our AMMPC method, at Moggill and Lowood the flow peaks are similar to those in [23] during the major event however there are no sudden jumps.

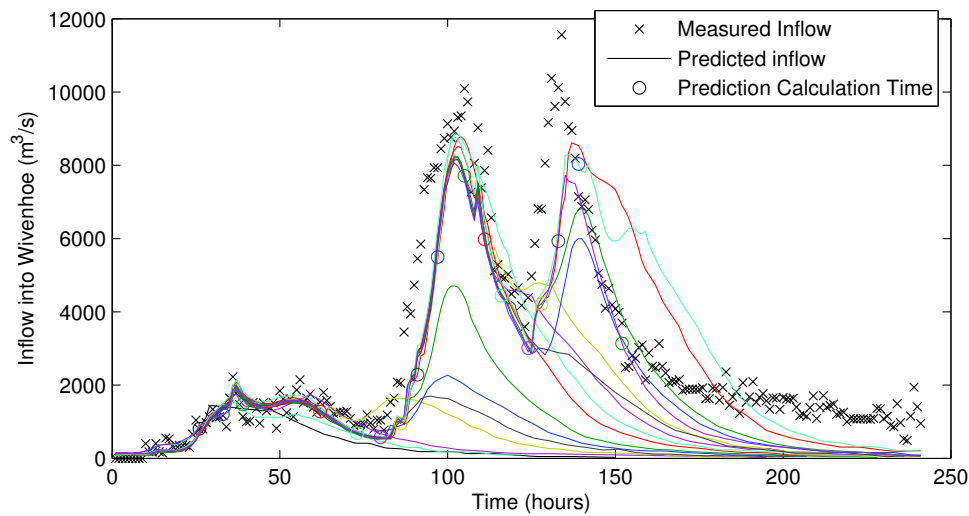


Fig. 9 Measured inflow and ensemble of predicted inflows into Wivenhoe reservoir. Each colored curve denotes an individual model run to predict the inflow

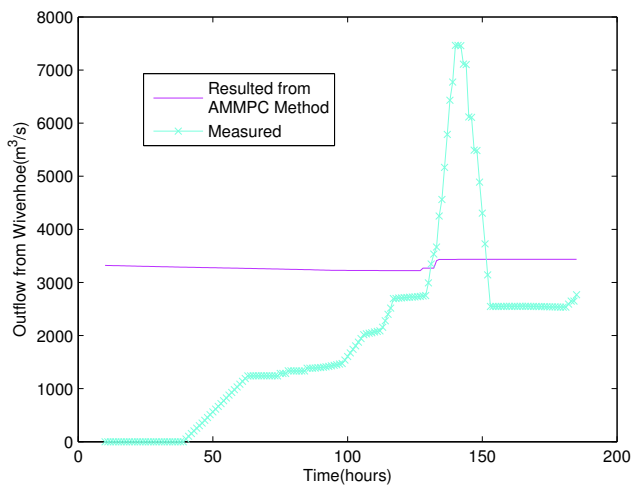


Fig. 10 Comparison of measured Wivenhoe outflow with that resulted by AMMPC method

5 Conclusion

A new solution called AMMPC, based on MMPC is proposed for predictive flood control in a regulated river system, in the presence of uncertain inflow conditions. It is different to the currently used methods in few ways. The disturbance set method considers all the disturbance events in the set equally likely and applies explicitly to the system model. Our AMMPC method describes the uncertainty as a bank of disturbance models and makes use of measurements to refine the control to match the

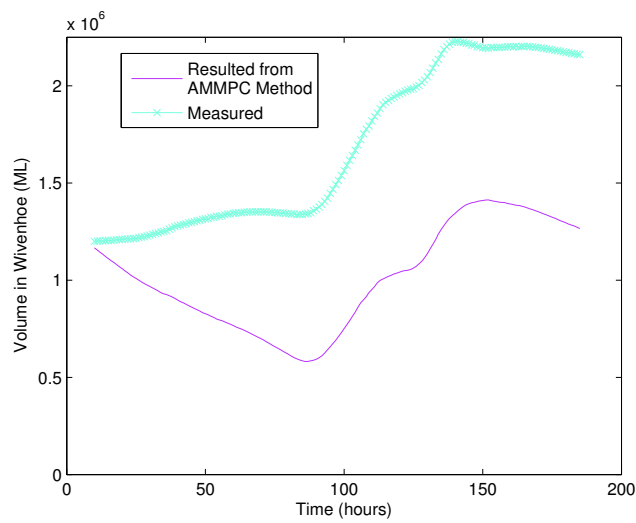


Fig. 11 Comparison of measured volume in Wivenhoe reservoir with that resulted by AMMPC method

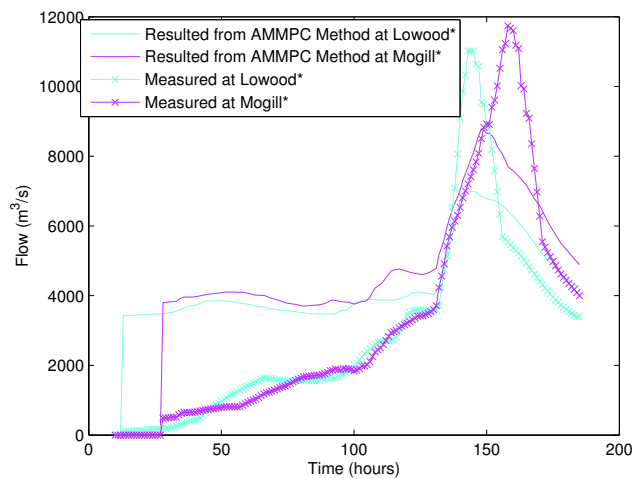


Fig. 12 Flows at Lowood and Moggill downstream the Wivenhoe reservoir. Both predicted and measured flows are approximate as there are no actual measurement data available for Lowood and Moggill but the most recent model predictions (predicted non-release flow). The total flow at a location is the predicted non-release flow plus predicted outflow (for AMMPC case) or measured outflow (for actual case)

actual model. Compared to MMPC methods in water control, it estimates the most likely model rather than using a-priori probabilities.

Firstly, we used a simple inflow model to demonstrate the performance of our AMMPC method for a hypothetical river network. Results indicate that our method adapts to the actual inflow condition rather than depending on a-priori knowledge. The inflows predicted from the URBS hydrological model for Wivenhoe reservoir during the 2011 Queensland floods were used in the second part of the simulations.

Results were compared with those obtained by the reservoir operational manual and a disturbance set method given in [23]. AMMPC method responds quicker than the both methods causing pre-release. As a result, it achieves 32% lower peak volume level than that resulted by the method in [23] while maintaining the same peak out-flow level. In addition to that, 99% of the inflow volume would be released by the end of the critical flood event which is in agreement with the dam operation requirements. Our AMMPC method was capable of obtaining a significant decrease in the peak volume and flow levels compared to the actual situation resulted by the reservoir operational scheme. The weights of the cost functions were tuned by trial and error method. In reality, the tuning should be done in advance, under normal flow conditions. These weights may be compared with the weights used in our simulations to calibrate the system for different flow conditions. In these simulations it was assumed that the measurement and process noise characteristics were known. However, in a critical flood event, noise can be introduced via sensor issues. Consequently, further research could be conducted on the effect of these noise characteristics.

References

1. Aldrighetti, E.: Computational hydraulic techniques for the saint venant equations in arbitrarily shaped geometry. Ph.D. thesis, University of Trento, Italy (2007)
2. Athans, M., Castagon, D., Dunn, K.P., Greene, C.S., Lee, W.H., Sandell, N.R., Willsky, A.S.: The stochastic control of the f-8c aircraft using a multiple model adaptive control (mmac) method- part i: Equilibrium flight. *IEEE Transactions on Automatic Control* **AC-22**(5), 768–779 (1977)
3. Blanco, T.B., Willems, P., Chiang, P.K., Haverbeke, N., Berlamont, J., Moor, B.D.: Flood regulation using nonlinear model predictive control. *Control Engineering Practice* **18**, 1147–1157 (2010)
4. Blanco, T.B., Willems, P., Moor, B.D., Berlamont, J.: Flood prevention of the demer using model predictive control. In: 17th IFAC World Congress (2007)
5. Block, P.J., Filho, F.A.S., Sun, L., Kwon, H.H.: A streamflow forecasting framework using multiple climate and hydrological models. *Journal of the American Water Resources Association* **45**, 828–843 (2009)
6. Breckpot, M., Blanco, T.B., Moor, B.D.: Flood control of rivers with model predictive control. In: American Control Conference (2010)
7. Breckpot, M., Blanco, T.B., Moor, B.D.: Flood control of rivers with nonlinear model predictive control and moving horizon estimation. In: 49th IEEE Conference on Decision and Control (CDC) (2010)
8. Burt, C.M., Mills, R.S., Khalsa, R.D., C., V.R.: Improved proportional-integral (pi) logic for canal automation. *Journal of Irrigation and Drainage Engineering* **124**, 53–57 (1998)
9. Chaudhry, M.H.: *Open Channel Flow*. Springer (2008)
10. Cheng, C., Wang, W., mei Xu, D., Chau, K.: Optimizing hydropower reservoir operation using hybrid genetic algorithm and chaos. *Water Resources Management* **22**, 895–909 (2008)
11. Chowdhury, S., Sharma, A.: Multisite seasonal forecast of arid river flows using a dynamic model combination approach. *Water Resources Research* **45**, 1–16 (2009)
12. Devineni, N., Sankarasubramanian, A., Ghosh, S.: Multimodel ensembles of streamflow forecasts: Role of predictor state in developing optimal combinations. *Water Resources Research* **44**, 1–22 (2008)
13. Ekeren, H.V., Negenborn, R., Overloop, P.V., Schutter, B.D.: Hybrid model predictive control using time-instant optimization for the rhine-meuse delta. Tech. rep., Delft Center for Systems and Control (2010)
14. Evans, R., Li, L., Mareels, I., Okello, N., Pham, M., Qiu, W., Saleem, S.K.: Real-time optimal control of river basin networks. In: Preprints of the 18th IFAC World Congress (2011)
15. Foo, M., Bedjaoui, N., Weyer, E.: Segmentation of a river using the saint venant equations. In: Control Applications (CCA), 2010 IEEE International Conference (2010)

16. Foo, M., Ooi, S.K., Weyer, E.: Modelling of river for control design. In: IEEE International Conference on Control Applications-Part of 2010 IEEE Multi-Conference on Systems and Control (2010)
17. Foo, M.F.L.: Modelling and control design of river systems. Ph.D. thesis, National ICT Australia, Department of Electrical and Electronic Engineering, The University of Melbourne (2012)
18. Fu, G., Butler, D., Khu, S.T.: Comparison of control strategies for multiobjective control of urban wastewater systems. In: 4th Biennial Meeting of iEMSs proceedings: International Congress on Environmental Modelling and Software, pp. 1347–1352. International Environmental Modelling and Software Society (2008)
19. Fu, G., Butler, D., Khu, S.T.: Multiple objective optimal control of integrated urban wastewater systems. *Environmental Modelling & Software* **23**(2), 225 – 234 (2008)
20. Gomez, M., Rodellar, J., Mantecon, J.A.: Predictive control method for decentralized operation of irrigation canals. *Applied Mathematical Modelling* **26**, 1039–1056 (2002)
21. Government of India Central Water Commission: Real Time Integrated Operation of Reservoirs-Reservoir Operation Directorate (2005)
22. Jakeman, A.J., Hornberger, G.M.: How much complexity is warranted in a rainfall-runoff model? *Water Resources Research* **29**, 2637–2649 (1993)
23. Kearney, M., Dower, P.M., Cantoni, M.: Model predictive control for flood mitigation: A wivenhoe dam case study. In: Australian Control Conference (2011)
24. L. Li, N.O., Pham, M., Saleem, S.K., Qiu, W., Evans, R., Mareels, I.: Model predictive control of murray-darling basin networks. In: Control and Decision Conference (2011)
25. Lakshmanan, V., Gourley, J.J., Flamig, Z., Giangrande, S.: A simple data-driven model for streamflow prediction. In: AMS Annual Meeting, Phoenix (2009)
26. Marinaki, M., Papageorgiou, M.: Optimal real time control of sewer networks. Springer (2005)
27. Ooi, S.K., E.Weyer: Control design for an irrigation channel from physical data. *Control Engineering Practice* **16**, 1132–1150 (2008)
28. Ooi, S.K., E.Weyer: Control design for an irrigation channel from physical data. *Control Engineering Practice* **16**, 1132–1150 (2008)
29. Ooi, S.K., Weyer, E.: Closed loop identification of an irrigation channel. In: Proceedings of the 40th IEEE Conference on Decision and Control (2001)
30. Overloop, P.J.V., Weijs, S., Dijkstra, S.: Multiple model predictive control on a drainage canal system. *Control Engineering Practice* **16**(5), 531 – 540 (2008)
31. Puig, V., Cembrano, G., Romera, J., Quevedo, J., Aznar, B., n, G.R., Cabot, J.: Predictive optimal control of sewer networks using coral tool: Application to riera blanca catchment in barcelona. *Water Science & Technology* **60**, 869–878 (2009)
32. Puig, V., Romera, J., Quevedo, J., Cardona, C.M., Salterain, A., Ayesa, E., Irizar, I., Castro, A., Lujan, M., Charbonnaud, P., Chiron, P., Trouvat, J.L.: Optimal predictive control of water transport systems: Art-darr/arrois case study. *Water Science and Technology* **60**, 2125–2133 (2011)
33. Ruiz, V.M., Ramirez, L.J.: Predictive control in irrigation canal operation. In: IEEE International Conference on Systems, Man, and Cybernetics (1998)
34. Schuurmans, J., Schuunnans, W., Berger, H., Meulenberg, M., Brouwe, R.: Control of water levels in the meuse river. *Journal of Irrigation and Drainage Engineering* **123**, 180–184 (1997)
35. SEQwater: January 2011 flood event-report on the operation of somerset dam and wivenhoe dam. Tech. rep., SEQwater (2011)
36. SEQwater: Manual of Operational Procedures for Flood Mitigation at Wivenhoe Dam and Somerset Dam (2011)
37. Wang, D., Salas, J.: Forecasting streamflow for colorado river systems. Tech. rep., Colorado Water Resources Research Institute (1991)
38. Wang, L.: Model Predictive Control system Design and Implementation Using Matlab, 1 edn. Springer-Verlag London Limited (2009)
39. Wang, L., Young, P.C.: Model predictive control design using non-minimal state space model. In: IFAC (2005)
40. Weyer, E.: System identification of an open water channel. *Control Engineering Practice* **9**, 1289–1299 (2001)
41. Weyer, E.: Control of irrigation channels. *IEEE Transactions on Control Systems Technology* **16**, 664–675 (2008)
42. Wu, C.L., Chau, K.: Data driven models for monthly streamflow time series predic. *Engineering Applications of Artificial Intelligence* **23**, 1350–1367 (2010)